

## Effect of electrode biasing on $m/n=2/1$ tearing modes in J-TEXT experiments

Hai Liu<sup>1</sup>, Qiming Hu<sup>1, a</sup>, Zhipeng Chen<sup>1, a</sup>, Q. Yu<sup>2</sup>, Lizhi Zhu<sup>1</sup>, Zhifeng Cheng<sup>1</sup>, Ge Zhuang<sup>1</sup> and Zhongyong Chen<sup>1</sup>

<sup>1</sup>State Key Laboratory of Advanced Electromagnetic Engineering and Technology, School of Electric and Electronic Engineering, Huazhong University of Science and Technology, 430074, Wuhan, People's Republic of China

<sup>2</sup>Max-Planck-Institut für Plasmaphysik, 85748 Garching, Germany

E-mail: [huqm@hust.edu.cn](mailto:huqm@hust.edu.cn) and [zpchen@hust.edu.cn](mailto:zpchen@hust.edu.cn)

**Abstract:** The effects of electrode biasing (EB) on the  $m/n = 2/1$  tearing mode have been experimentally studied in J-TEXT tokamak discharges, where  $m$  and  $n$  are the poloidal and toroidal mode numbers. It is found that for a negative bias voltage, the mode amplitude is reduced, and the mode frequency is increased accompanied by the increased toroidal plasma rotation speed in the counter- $I_p$  direction. For a positive bias voltage, the mode frequency is decreased together with the change of the rotation velocity towards the co- $I_p$  direction, and the mode amplitude is increased. Statistic results show that the variations in the toroidal rotation speed, the  $2/1$  mode frequency and its amplitude linearly depend on the bias voltage. The threshold voltages for complete suppression and locking of the mode are found. The experimental results suggest that applied electrode biasing is a possible method for the avoidance of mode locking and disruption.

**Keywords:** Tearing mode, electrode biasing, plasma rotation, mode stabilization/destabilization.

### 1. Introduction

It is well known that the onset of the tearing modes (TM) or neoclassic tearing modes (NTM) can degrade the tokamak confinement. Once the mode amplitude is sufficiently large, mode locking and major disruption will happen, being an important issue to be solved for a fusion reactor. Extensive theoretical and experimental studies have been carried out before to study the mode stability, the onset conditions of the mode and the mode stabilization by localized current drive or heating. In addition, disruption avoidance by stabilizing the TM has also attracted much research efforts.

Among these studies, the effect of plasma flow (or rotation) on the TM is of great interest [1]. For a low edge safety factor, the mode stability is found to depend more on the plasma velocity at the resonant surface rather than on the flow shear, and a sufficiently high plasma rotation speed can also stabilize the resistive wall mode [2]. The flow shear is considered to affect MHD modes and the shape of magnetic islands [3-9]. It is shown later that depending on the plasma parameters, plasma flow shear can either increase or decrease the TM growth rate [3-12]. Recent numerical simulation reveals that a larger plasma rotation speed results in a smaller TM growth rate in the linear phase and a smaller saturated island in the nonlinear phase [10].

In experiments it is generally found that with decreasing the plasma rotation, the TM is more unstable and the saturated islands become larger [13-15]. Several methods have been utilized in experiments to vary the plasma flow and to investigate its effect on MHD instabilities. The varying mix of co- and counter-neutral beams injection (NBI) is applied to change the rotation on DIII-D and JT-60U, showing that the shear flow has a stabilizing effect on  $m/n = 3/2$  NTM ( $m$  and  $n$  are the poloidal and toroidal mode numbers) [16-18]. The normalized beta limit for the  $m/n = 2/1$  NTM onset decreases as the co-torque is removed [19]. On NSTX, the rotation is varied by the

<sup>a</sup> Authors to whom any correspondence should be addressed.

application of  $n = 3$  static magnetic perturbation, and a stabilizing effect from the rotation shear is found [20]. On JET, the plasma rotation is also found to stabilize the  $m/n = 3/2$  mode [21]. On T-10, the frequency and amplitude of MHD modes are found to be able controlled by a non-disruptive halo-current [22]. In some medium or small size tokamaks, the biased electrode is an efficient method to change the plasma parameters and flows [23-28]. Suppression of MHD activity with electrode [28] or limiter biasing [26] has been observed in experiments. The sheared poloidal rotation generated by biased electrode is shown to decrease the linear stability index  $\Delta'$  [27].

Motivated by existing experimental and numerical results, an electrode biasing (EB) system for driving plasma rotation has been designed and installed on J-TEXT tokamak, being able to insert into the plasma by a reciprocating drive during the discharge [29-31]. Experiments have been carried out to change the edge plasma rotation by using EB and to study the corresponding effect on the  $m/n = 2/1$  TM, as presented in this paper. It is found that, the TM is accelerated (decelerated) and stabilized (destabilized) with negative (positive) bias, along with increasing (decreasing) of plasma rotation in counter- $I_p$  direction. The stabilizing (destabilizing) effect on TM linearly depends on the value of the negative (positive) bias voltage. The TM is completely suppressed when the negative bias voltage reaches about -300 V, and mode locking is triggered when the positive bias voltage reaches to about +110 V. Periodical stabilization (destabilization) of TM by modulated negative (positive) EB is also observed in experiments.

This paper is organized as follows: the experimental setup is introduced in subsection 2.1; the influences of EB on  $m/n = 2/1$  TM are presented in subsection 2.2, including different bias voltages with both negative and positive polarities; A brief discussion and summary are presented in section 3.

## 2. Experimental setup and results

### 2.1. Experimental setup

The experiments reported in this paper are carried out in Ohmic hydrogen discharges on J-TEXT tokamak with a limiter configuration (major radius  $R_0 = 105$  cm and minor radius  $a = 25.5$  cm) [32]. Unless otherwise stated, the experimental results presented below were carried out during the 2015 Autumn experimental campaign, and the plasma parameters are as follows: plasma current  $I_p = 165$  kA, toroidal magnetic field  $B_t = 1.6$  T, the safety factor  $q_a = 3$  at the plasma edge, and the central line-averaged electron density  $n_e \sim 1.1\text{--}1.2 \times 10^{19} \text{ m}^{-3}$ . In these discharges an  $m/n = 2/1$  TM grows and saturates before the application of EB, and this mode rotates in the electron diamagnetic drift direction with a frequency of 5 kHz.

The electrode biasing system [30] is installed at a mid-plane port on the low field side (LFS), as shown in figure 1(a). A disc shaped (1.3 cm in thickness and 4 cm in diameter) graphite electrode is mounted on the head of the EB and inserted into the plasma by a reciprocating drive during the discharge at the location of  $r = 23.5$  m, that is 2 cm inside the last closed flux surface (LCFS). The bias voltage  $U_{EB}$  applied on the electrode with respect to the limiter (or vacuum vessel wall) is in the range of -300 to +120 V. The corresponding volt-ampere characteristic of the EB in the presence of the  $m/n = 2/1$  TM is shown in figure 1(b), which shows that the EB current  $I_{EB}$  is proportional to the bias voltage  $U_{EB}$ . The positive  $I_{EB}$  means the current flows out of the electrode. The maximum input power of the EB ( $\sim 18$  kW) is less than 6% of the Ohmic heating power ( $\sim 300$  kW), thus the heating effect of EB on plasma can be ignored. It is known [33] that the EB could produce radial current density  $J_r$  between the electrode-located flux surface and

LCFS, yielding the  $J_r \times B_\theta$  ( $J_r \times B_t$ ) torque to change the toroidal (poloidal) plasma rotation. On J-TEXT, the spontaneous toroidal rotation inside  $r/a = 0.8$  is usually in the counter- $I_p$  direction. The negative (positive)  $I_{EB}$  corresponds to the radially inward (outward) current density. The toroidal plasma rotation speed is therefore expected to increase (decrease) with negative (positive) bias.

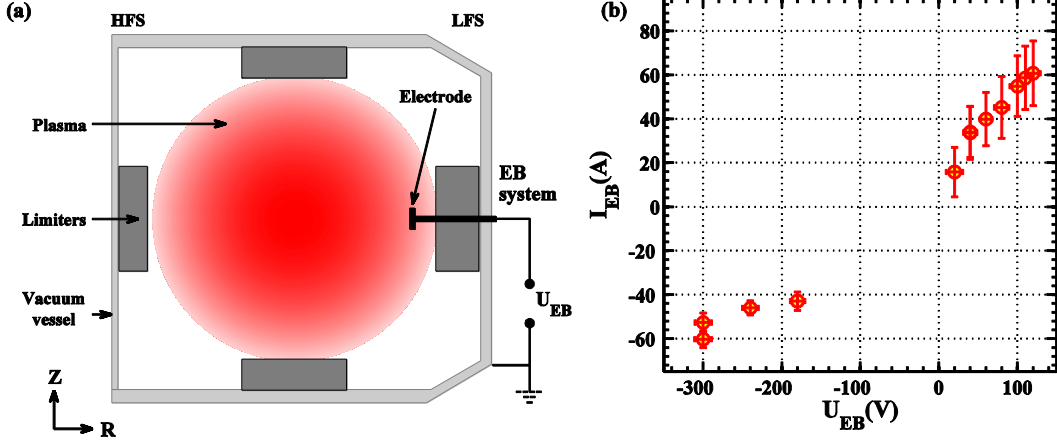


**Figure 1.** (a) Cross-section of J-TEXT and the layout of electrode biasing system. (b) Volt-ampere characteristic of the electrode biasing in the presence of  $m/n = 2/1$  tearing mode.

The edge toroidal rotation of Carbon V (i.e.  $C^{+4}$ ) impurity is measured by the multi-channel spectrometer [34] in the range of  $r/a = 0.65 \sim 1$ . The  $m/n = 2/1$  TM is measured by poloidal and toroidal Mirnov arrays and identified from the temporal evolution of the Mirnov signals using singular value decomposition (SVD) technique [35]. The locked mode detectors consist of two sets of saddle loops. Each set contains two loops installed at two opposite toroidal locations outside of the vacuum vessel. The difference between the signals from two saddle loops in one set shows the radial magnetic perturbation  $\delta B_r$  with odd toroidal mode number ( $n = 1, 3, 5, \dots$ ). The  $q = 2$  rational surface is at about  $r \sim 19$  cm (i.e.  $r/a = 0.74$ ), which is estimated by the reverse radius of electron temperature perturbation measured by electron cyclotron emission (ECE) [36].

## 2.2. Experimental results

Two examples of the effect of bias on the  $2/1$  TM are shown in figure 2. The bias voltages are  $U_{EB} = -300$  V and  $+80$  V for shots 1042698 and 1042707, respectively. Figure 2(a) shows the plasma currents of these two shots. Figure 2(b) displays the location of the electrode during its movement, which begins to move from  $\Delta r_{EB} = 3$  cm into the plasma at  $t = 0.2$  s, goes through the LCFS at about 0.26 s and stays at  $\Delta r_{EB} = -2$  cm from 0.3 to 0.6 s, where  $\Delta r_{EB}$  is the EB location with respect to LCFS. When the EB is inserted into plasma before applying bias voltage during the time interval of  $0.26 \text{ s} < t < 0.3 \text{ s}$ , there is a minor effect on the plasma. The TM frequency is decreased from 5 to 4 kHz, and mode amplitude is slightly increased as indicated by the evolution of the mode frequency  $f_{MHD}$  and poloidal perturbation magnetic  $\delta B_\theta$  shown in figure 2(g) to 2(j). The electron density  $n_e$  is slightly increased (figure 2(f)).

The bias voltage is turned on at  $t = 0.33$  s, ramped up to the flattop at  $t = 0.34$  s and turned off at  $t = 0.45$  s, as shown in figure 2(c). For shot 1042698, when turning on the bias with negative voltage  $U_{EB} = -300$  V at the flattop, the bias current  $I_{EB}$  ramps up to about  $-60$  A as shown in figure 2(d). In the time interval of  $0.33 \text{ s} < t < 0.39$  s, the frequency of  $2/1$  TM increases from 4 to 8 kHz, while the magnetic perturbation amplitude of the  $2/1$  TM is suppressed from 0.9 mT to noise level. Meanwhile, the electron density  $n_e$  is increased, while  $H_\alpha$  signals are decreased,

revealing the improved particle confinement. In the time interval of  $0.425 \text{ s} < t < 0.45 \text{ s}$ , both the  $I_{\text{EB}}$  and electron density  $n_e$  increase rapidly due to the overheating of the electrode and the releasing of impurity. As a result, the plasma parameters change substantially, and the 2/1 TM does not appear again when turning off the bias voltage at  $t = 0.45 \text{ s}$ . For shot 1042707 with a positive voltage  $U_{\text{EB}} = +80 \text{ V}$  at the flattop, the bias current is about 45 A as shown in figure 2(c) and 2(d). The mode frequency is slowed down from 4 to 1 kHz, and  $\delta B_\theta$  is increased from 1 to 1.8 mT. The electron density  $n_e$  and  $H_\alpha$  signals change little. When turning off the bias voltage at  $t = 0.45 \text{ s}$ , the 2/1 TM recovers to its initial state. Figure 2 reveals that negative bias increases the frequency of the 2/1 TM and stabilizes the mode, while the positive bias leads to the opposite results.

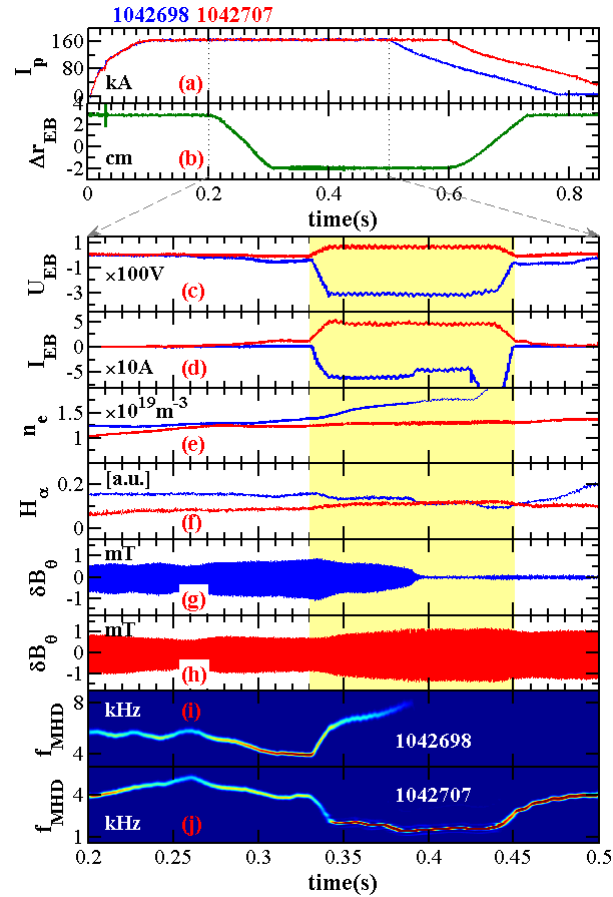


**Figure 2.** Time evolutions of (a) plasma current ( $I_p$ ), (b) location of the electrode ( $\Delta r_{\text{EB}}$ ), (c) EB voltage ( $U_{\text{EB}}$ ), (d) EB current ( $I_{\text{EB}}$ ), (e) central line-averaged electron density ( $n_e$ ), (f)  $H_\alpha$  radiation level ( $H_\alpha$ ), (g)/(h) poloidal magnetic perturbation ( $\delta B_\theta$ ) and (i)/(j)  $m/n = 2/1$  TM frequency ( $f_{\text{MHD}}$ ) for shots 1042698 and 1042707.

Corresponding to figure 2, the time evolutions of the toroidal rotation  $V_\phi$  of Carbon impurity at different radial locations ( $r/a = 0.96, 0.89, 0.82, 0.74, 0.66$ ) are shown in figure 3(a)-3(e), where the positive value corresponds to the co- $I_p$  direction. The toroidal rotation speed increases (decreases) in the counter- $I_p$  direction with negative (positive) bias, as shown by blue circles (red squares) in figure 3(a)-3(e). Figure 3(f) shows the radial profiles of the toroidal rotation velocity  $V_\phi$ . The solid/dotted lines are time-averaged profiles with/before bias, respectively. The radial profiles of the relative variations of rotation speed before and with bias,  $\Delta V_\phi$ , are shown in figure 3(g), here the positive value means rotation increases in the co- $I_p$  direction. Corresponding to figure 3(f), the profiles of the velocity shear  $dV_\phi/dr$  are shown in figure 3(h), which are averaged

from the differential of the velocity profiles (the cubic spline interpolation of the profiles is adopted before differential). Before bias, the rotation velocity and its shear in the island region ( $r/a \sim 0.74$ ) for these two discharges are almost the same ( $\sim -5$  km/s and  $\sim 1.5 \times 10^5$  s $^{-1}$ ). After turning on the bias, the changes of rotation velocity and its shear are opposite: increasing to  $-18$  km/s and  $2.8 \times 10^5$  s $^{-1}$  for negative bias but decreasing to  $+5$  km/s and  $0.8 \times 10^5$  s $^{-1}$  for positive bias.

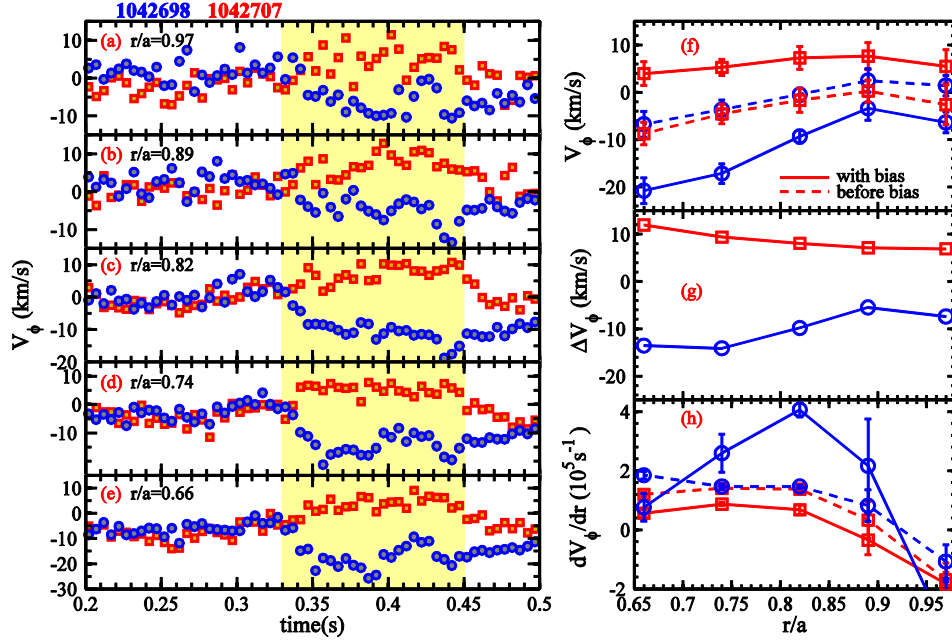


**Figure 3.** Time evolutions of (a) to (e) Carbon V toroidal rotation velocity  $V_\phi$  at different radial locations and time-averaged data of radial profiles of (f) rotation velocity, (g) variations of rotation velocity and (h) rotation velocity shear before and with bias.

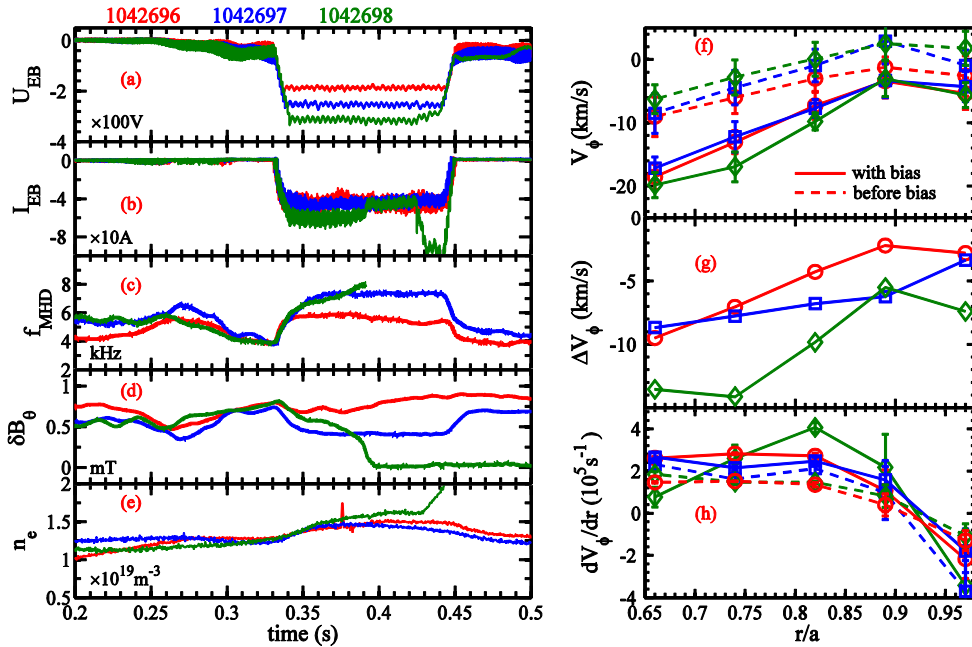


**Figure 4.** Effect of different negative bias voltages on tearing mode. Time evolutions of (a) EB voltage ( $U_{EB}$ ), (b) EB current ( $I_{EB}$ ), (c)  $m/n = 2/1$  TM frequency ( $f_{MHD}$ ), (d) poloidal magnetic perturbation ( $\delta B_\theta$ ), and (e) central line-averaged electron density ( $n_e$ ). Time-averaged data of (f) radial profiles of rotation velocity, (g) variations of rotation velocity and (h) rotation velocity shear before and with bias.

With increasing the bias voltage  $U_{EB}$  (figure 4(a)) and hence bias currents  $I_{EB}$  (figure 4(b)), the effect of different negative bias voltages on the  $2/1$  TM is shown in figure 4. For shot 1042696

with bias voltage -180 V, the TM frequency is increased from 4 to 6 kHz, and  $\delta B_\theta$  is decreased from 0.9 to 0.7 mT. Here, the magnetic perturbations  $\delta B_\theta$  indicates the envelope of poloidal magnetic perturbations. Increasing the bias voltage to -240 V in shot 1042697,  $f_{\text{MHD}}$  and  $\delta B_\theta$  are further changed to 7.8 kHz and 0.4 mT. The mode is completely stabilized in shot 1042698 with a bias voltage -300 V. The radial profiles of the toroidal rotation velocity, variations of rotation velocity due to bias and the rotation velocity shear are shown in figure 4(f)-(h). A higher negative bias voltage causes a larger increase in the plasma rotation speed, as expected.

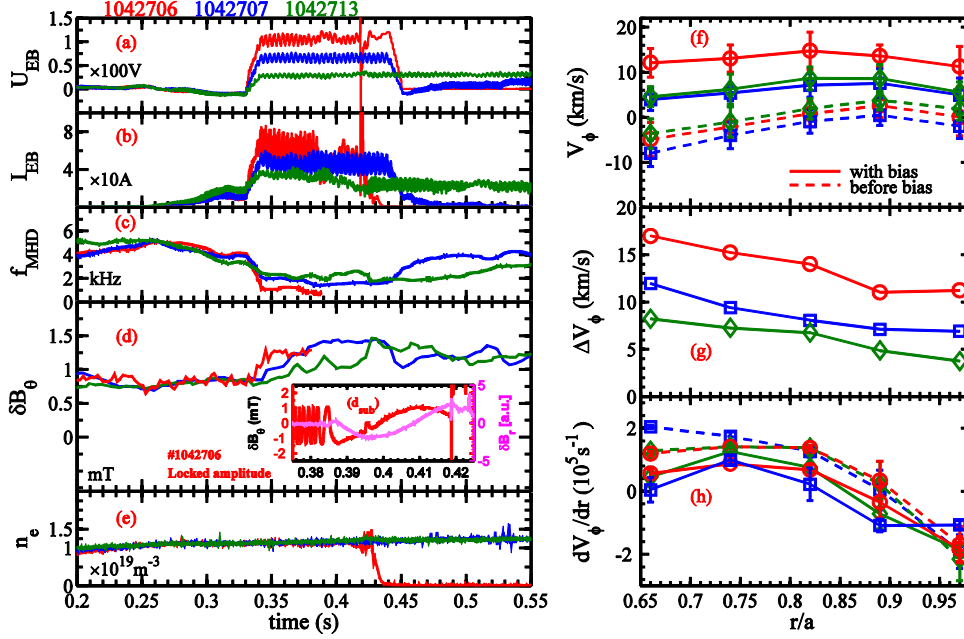


**Figure 5.** Effect of different positive bias voltages on tearing mode. Time evolutions of (a) EB voltage ( $U_{\text{EB}}$ ), (b) EB current ( $I_{\text{EB}}$ ), (c)  $m/n = 2/1$  TM frequency ( $f_{\text{MHD}}$ ), (d) poloidal magnetic perturbation ( $\delta B_\theta$ ), and (e) central line-averaged electron density ( $n_e$ ). Time-averaged data of (f) radial profiles of rotation velocity, (g) variations of rotation velocity and (h) rotation velocity shear before and with bias. In figure 5(d), the subgraph ( $d_{\text{sub}}$ ) shows the time evolution of poloidal magnetic perturbation  $\delta B_\theta$  and the locked mode detector signal  $\delta B_r$  in the time interval of  $0.375 \text{ s} < t < 0.425 \text{ s}$ , which clearly shows the happening of mode locking.

In figure 5, discharges with different positive voltages are shown. In opposite to the results of negative bias, for positive bias the TM frequency is decreased from 4 to 2.5 kHz and  $\delta B_\theta$  is increased from 1 to 1.1 mT for the bias voltage  $U_{\text{EB}} = +40 \text{ V}$  at the flattop (shot 1042713). For shot 1042707 with  $U_{\text{EB}} = +80 \text{ V}$ ,  $f_{\text{MHD}}$  and  $\delta B_\theta$  are further changed to 1.5 kHz and 1.5 mT, indicating that the higher positive bias voltage has stronger decelerating and destabilizing effects on the 2/1 TM. For the bias voltage +120 V (shot 1042706), mode locking happens after the mode frequency slowed down to 0.8 kHz at  $t = 0.39 \text{ s}$ , and this leads to disruption at  $t = 0.42 \text{ s}$ . Figure 5(d) shows the amplitude of  $\delta B_\theta$  for shot 1042706 just before mode locking. A subgraph ( $d_{\text{sub}}$ ) displays the time evolution of the poloidal magnetic perturbation  $\delta B_\theta$  and the locked mode detector signal  $\delta B_r$  in the time interval of  $0.375 \text{ s} < t < 0.425 \text{ s}$ , which clearly shows the happening of mode locking. The rotation velocity profiles, variations of rotation velocity and the velocity shear are changed more obvious for higher bias voltage, as shown in figure 5(f)-(h).

In figures 4 and 5, the 2/1 TM recovers after turning off the EB, unless it is completely suppressed or locked. To study whether this process is repeatable, modulated bias waveforms are applied, as shown in figure 6. The amplitudes of the periodic bias voltages are -240 V for shot 1042702 and +80 V for shot 1042711, which are not high enough to lead to complete suppression



or locking of the 2/1 TM. Periodic stabilization/destabilization of TM (figure 6(c)) are seen together with the increase/decrease of the TM frequency (figure 6(b)) for negative/positive bias voltage. In addition, the plasma parameters ( $n_e$  and  $H_\alpha$ ) and toroidal rotation velocity (at  $r/a = 0.74$ ) also vary periodically, implying that the plasma particle confinement and plasma rotation are also modulated. The bias voltage  $U_{EB}$  ramps up to the flat-top in 1 ms, and the TM frequency also increases (decreases) 1.5 kHz in 1 ms, being much faster than change of other plasma parameters.

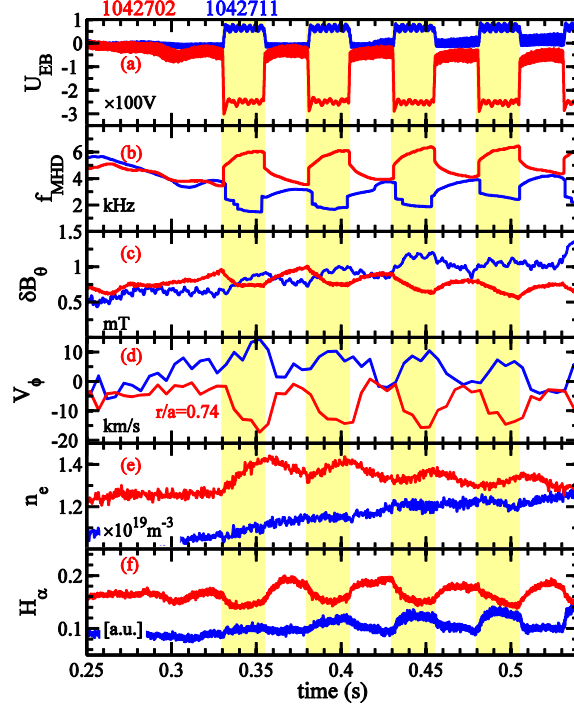


**Figure 6.** Effect of modulated of bias on tearing modes. Time evolutions of (a) EB voltage ( $U_{EB}$ ), (b)  $m/n = 2/1$  TM frequency ( $f_{MHD}$ ), (c) poloidal magnetic perturbation ( $\delta B_\theta$ ), (d) toroidal rotation velocity at  $r=0.74a$ , (e) central line-averaged electron density ( $n_e$ ), and (f)  $H_\alpha$  radiation level ( $H_\alpha$ ).

The periodic recovery of the plasma rotation and TM frequency can be attributed to the flow damping. Study of momentum transport and flow damping in the Madison Symmetric Torus (MST) indicated that the plasma flow caused by the EB could be damped in  $\sim 2.5$  ms after turning off EB, being much shorter than the predicted time by classical theory ( $\sim 250$  ms) [37]. That means the effect of plasma flow variation (caused by EB) on the TM can be quickly removed when turning off the bias.

Systematical experiments have been carried out by keeping the background plasma parameters to be the same, while only the bias voltage is scanned from -300 to +120 V. In figure 7(a), (b) and (c), the variations of rotation velocity ( $\Delta V_\phi$ ) at  $r/a = 0.74$ , TM frequency ( $f_{MHD}$ ), and the normalized poloidal magnetic perturbation ( $\delta B_{\theta,nor}$ ) of the 2/1 TM are shown as a function of the EB voltage, respectively. Here  $\delta B_{\theta,nor} = \delta B_\theta / \delta B_{\theta 0}$ ,  $\delta B_{\theta 0}$  is the initial amplitude of poloidal magnetic perturbation before biasing, and  $\delta B_\theta$  is the amplitude of poloidal magnetic perturbation in steady state during the application of EB.  $\Delta V_\phi > 0$  ( $< 0$ ) means the plasma rotation accelerates in co-(counter-)  $I_p$  direction.  $\delta B_{\theta,nor} < 1$  ( $> 1$ ) corresponds to the stabilization (destabilization) of 2/1 TM. The blue stars with red face in figure 7 are the results obtained in 2015 autumn-campaign. When changing  $U_{EB}$  from -180 to -300 V, the rotation speed increment (in counter- $I_p$  direction) in the island region changes from 7 to 14 km/s,  $f_{MHD}$  increases from 6 to 8 kHz, and  $\delta B_{\theta,nor}$  decreases from 1 to 0. When increasing  $U_{EB}$  from +20 to +120 V, the rotation speed increment (in co- $I_p$  direction) in the island region changes from 2 to 15 km/s,  $f_{MHD}$  decreases from 4 to 0.8 kHz, and

$\delta B_{\theta, \text{nor}}$  increases from 1 to 1.7. The relationship between  $U_{EB}$  and  $\delta B_{\theta, \text{nor}}$  (figure 7(c)) indicates that the stabilization/destabilization effect on TM linearly depends on the value of bias voltage. Further experiments have been carried out in 2016 Spring experimental campaign (parameters:  $I_p = 175$  kA,  $B_t = 1.6$  T,  $q_a = 2.8$  and  $n_e \sim 1.5 \times 10^{19} \text{ m}^{-3}$ ), and the results are also shown in figure 7(b) and (c) by red circles with yellow face, which agree well with that obtained in 2015, showing the linear dependence of  $f_{\text{MHD}}$  and  $\delta B_{\theta, \text{nor}}$  on the bias voltage.

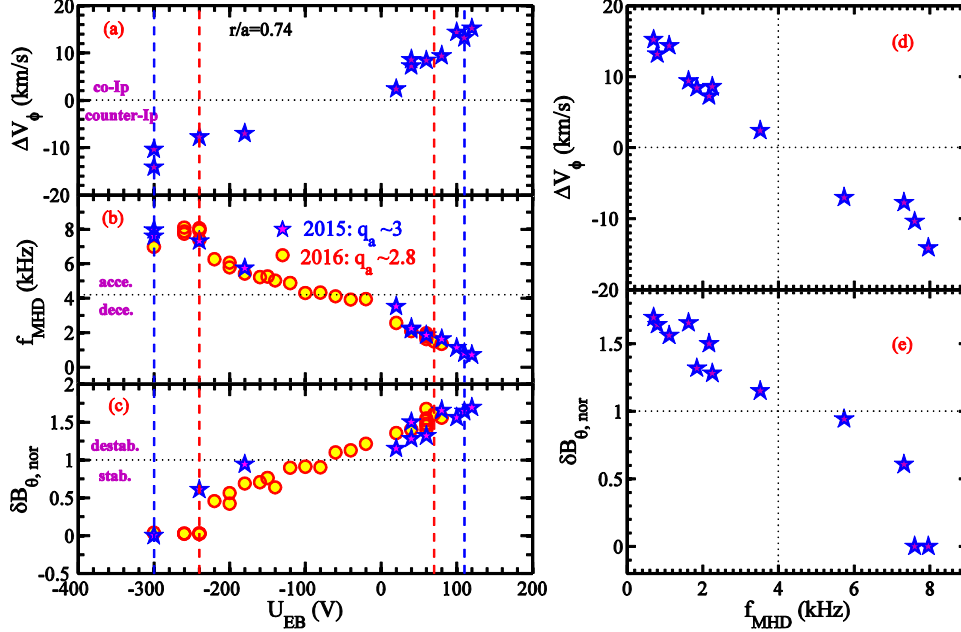


**Figure 7.** The statistical results of (a) the variation of rotation at  $r/a = 0.74$ , (b) TM frequency  $f_{\text{MHD}}$  and (c) normalized poloidal magnetic perturbation  $\delta B_{\theta, \text{nor}}$  versus bias voltage.  $\delta B_{\theta, \text{nor}} = \delta B_\theta / \delta B_{00}$ ,  $\delta B_{00}$  and  $\delta B_\theta$  are the initial and steady amplitude of the poloidal magnetic perturbation before and during the application of EB, respectively. (d) and (e) show  $\Delta V_\phi$  and  $\delta B_{\theta, \text{nor}}$  as a function of  $f_{\text{MHD}}$ .

There exists a threshold bias voltage for complete suppression or locking of the 2/1 TM. For the plasmas in 2015 Autumn experimental campaign, the thresholds are about -300 V (with  $I_{EB} \sim -60$  A) and +110 V (with  $I_{EB} \sim 60$  A) for complete suppression and locking of TM, respectively. While for the plasmas in 2016 Spring experimental campaign, they are -240 V (with  $I_{EB} \sim -40$  A) and +70 V (with  $I_{EB} \sim 40$  A). The magnetic island is closer to the EB source in 2016 experiments due to a lower value of  $q_a$  ( $q_a = 2.8$ ). It is noticed that for both campaigns, the TM frequencies before complete mode suppression are almost the same ( $\sim 8$  kHz), and the values of  $\delta B_{\theta, \text{nor}}$  for mode locking are also close ( $\sim 1.7$ ). Figures 7(d) and (e) show the values of  $\Delta V_\phi$  and  $\delta B_{\theta, \text{nor}}$  as a function of  $f_{\text{MHD}}$ . Both  $\Delta V_\phi$  and  $\delta B_{\theta, \text{nor}}$  have a linear dependence on  $f_{\text{MHD}}$ , revealing that the change of TM amplitude and frequency is associated with variation of plasma rotation by bias voltage.

### 3. Discussion and summary

The effects of electrode biasing on the  $m/n=2/1$  TM have been studied in J-TEXT tokamak experiments. As expected, the negative (positive) bias accelerates (decelerates) the rotation of 2/1 TM and stabilizes (destabilizes) the mode. The toroidal plasma rotation speed is increased (decreased) in the counter- $I_p$  direction for negative (positive) bias. There is a linear dependence of the changes of plasma rotation velocity, the mode frequency and mode amplitude on the bias voltage. These results indicate that the TM amplitude can be affected by the rotation speed or its shear, being stabilized once the mode frequency is high enough. The threshold voltages of EB for complete mode suppression are about -300 V (-240 V) for  $q_a = 3$  ( $q_a = 2.8$ ). It is therefore expected



that an EB system, being able to insert into the plasma by a reciprocating drive before mode locking, is a possible method for speeding up the TM rotation and for the avoidance of mode locking and subsequent disruption. Experiments on this subject will be carried out on J-TEXT in the near future.

Our experimental results are consistent with the findings in other tokamak experiments [e.g. 16-18] as well as numerical results [10] that a stronger shear plasma flow stabilizes the TM. It is impossible to distinguish the effects of rotation speed ( $V_\phi$ ) and rotation shear ( $dV_\phi/dr$ ) on the TM mode in our experiments, since both increase (decrease) with negative (positive) bias voltage. Results shown in figure 6 reveal that the mode frequency  $f_{\text{MHD}}$  changes much faster than the toroidal rotation speed  $V_\phi$  when turning on/off the EB voltage, indicating that  $f_{\text{MHD}}$  may decouple from  $V_\phi$ . One possible explanation is that EB also changes the poloidal rotation velocity in addition to the toroidal one, and which affects the mode frequency. Measurement of the poloidal rotation velocity is still needed and will be carried out in future experiment.

In summary, both negative and positive bias voltages are utilized to affect the 2/1 TM in J-TEXT Ohmic plasmas. The major results are as follows:

- (1) Negative (positive) bias accelerates and stabilizes (decelerates and destabilizes) the 2/1 TM.
- (2) Plasma rotation speed and its shear are increased (decreased) with negative (positive) bias.
- (3) The changes in the rotation speed, the 2/1 mode frequency and amplitude linearly depend on the bias voltage. A bias voltage of -300 V or -240 V (+110 V or +70 V) causes complete suppression (locking) of 2/1 TM. The threshold voltages are affected by the q-profile.
- (4) Periodic acceleration and stabilization (deceleration and destabilization) of the 2/1 TM by modulated negative (positive) bias are observed in discharges.

## Acknowledgments

The authors would like to thank the members of the J-TEXT team for their assistance in the experiment. This work is supported by National Magnetic Confinement Fusion Science Program of China under contract No. 2015GB111001 and the National Natural Science Foundation of China (Contract No. 11305070 and 11505069).

## References

- [1] Frieman E. and Rotenberg M. 1960 *Rev. Mod. Phys.* **32** 898
- [2] Chu M. S. *et al* 1995 *Phys. Plasmas* **2** 2236
- [3] Wei L. and Wang Z. X. 2013 *Phys. Plasmas* **20** 012512
- [4] Chapman I. T. *et al* 2012 *Nucl. Fusion* **52** 042005
- [5] Wang X. *et al* 1998 *Phys. Plasmas* **5** 2291
- [6] Bierwage A. *et al* 2007 *Phys. Plasmas* **14** 010704
- [7] Ofman L. *et al* 1991 *Phys. Fluids B: Plasma Phys.* **3** 1364
- [8] Chen X. L. and Morrison P. J. 1990 *Phys. of Fluids B: Plasma Phys.* **2** 495
- [9] Chu M. S. *et al* 1999 *Nucl. Fusion* **39** 2107
- [10] Hu Q. *et al* 2014 *Phys. Plasmas* **21** 122507
- [11] Chandra D. *et al* 2005 *Nucl. Fusion* **45** 524
- [12] Coelho R. and Lazzaro E. 2007 *Phys. Plasmas* **14** 012101

- [13] Ono M. *et al* 2000 *Nucl. Fusion* **40** 557
- [14] Luxon J. L. 2002 *Nucl. Fusion* **42** 614
- [15] Keilhacker M. and the JET Team 1999 *Plasma Phys. Control. Fusion* **41** B1
- [16] La Haye R. J. and Buttery R. J. 2009 *Phys. Plasmas* **16** 022107
- [17] La Haye R. J. *et al* 2010 *Phys. Plasmas* **17** 056110
- [18] La Haye R. J. *et al* 2011 *Nucl. Fusion* **51** 053013
- [19] Buttery R. J. *et al* 2008 *Phys. Plasmas* **15** 056115
- [20] Gerhardt S. P. *et al* 2009 *Nucl. Fusion* **49** 032003
- [21] Cheetham A. D. *et al* 1987 *Nucl. Fusion* **27** 843
- [22] Chudnovskiy A. N. *et al* 2003 *Nucl. Fusion* **43** 681
- [23] Taylor R. J. 1985 *Nucl. Fusion* **25** 1173
- [24] Taylor R. J. *et al* 1989 *Phys. Rev. Lett.* **63** 2365
- [25] Ghoranneviss M. *et al* 2010 *J.Fusion Energ.* **29** 467
- [26] Lu H. W. *et al* 2012 *Eur. Phys. J. D* **66** 213
- [27] Dhyani P. *et al* 2014 *Nucl. Fusion* **54** 083023
- [28] Nascimento I. C. *et al* 2007 *Nucl. Fusion* **47** 1570
- [29] Sun Y. *et al* 2016 *Nucl. Fusion* **56** 046006
- [30] Zhu T. Z. *et al* 2014 *Rev. Sci. Instrum.* **85** 053504
- [31] Sun Y. *et al* 2014 *Plasma Phys. Control. Fusion* **56** 015001
- [32] Zhuang G. *et al* 2015 *Nucl. Fusion* **55** 104003
- [33] Askinazi L. G. *et al* 1992 *Nucl. Fusion* **32** 271
- [34] Cheng Z. F. *et al* 2014 *Rev. Sci. Instrum.* **85** 11E423
- [35] Raju D. *et al* 2000 *Pramana-J. Phys.* **55** 727
- [36] Yang Z. J. *et al* 2012 *Rev. Sci. Instrum* **83** 10E313
- [37] Almagri A. F. *et al* 1998 *Phys. Plasmas* **5** 3982